CubeSat deformable mirror demonstration

Citation: Cahoy, Kerri, Anne Marinan, Caitlin Kerr, Kezi Cheng, and Sara Jamil. “CubeSat deformable mirror demonstration.” In Space Telescopes and Instrumentation 2012: Optical, Infrared, and Millimeter Wave, 84424F-84424F-11. SPIE - International Society for Optical Engineering, 2012. © 2012 Society of Photo-Optical Instrumentation Engineers (SPIE)

Published Version: http://dx.doi.org/10.1117/12.926681

Publisher:

Permanent Link: http://hdl.handle.net/1721.1/80847

Version: Final published version: final published article, as it appeared in a journal, conference proceedings, or other formally published context

CubeSat Deformable Mirror Demonstration

Kerri Cahoy*[a], Anne Marinan[a], Caitlin Kerr[a], Kezi Cheng[a], Sara Jamil[b]
[a]Department of Aeronautics and Astronautics, Massachusetts Institute of Technology, 77 Mass. Ave., Cambridge, MA, USA 02139; [b]Institut Supérieur de l'Aéronautique et de l'Espace, 10 av. Edouard Belin, Toulouse, France, 54032-31055

ABSTRACT

The goal of the CubeSat Deformable Mirror Demonstration (DeMi) is to characterize the performance of a small deformable mirror over a year in low-Earth orbit. Small form factor deformable mirrors are a key technology needed to correct optical system aberrations in high contrast, high dynamic range space telescope applications such as space-based coronagraphic direct imaging of exoplanets. They can also improve distortions and reduce bit error rates for space-based laser communication systems. While follow-on missions can take advantage of this general 3U CubeSat platform to test the on-orbit performance of several different types of deformable mirrors, this first design accommodates a 32-actuator Boston Micromachines MEMS deformable mirror.

Keywords: deformable mirrors, wavefront control, CubeSat, MEMS, adaptive optics, space telescopes, coronagraph, exoplanets

1. INTRODUCTION

Ground-based adaptive optics systems that utilize deformable mirrors were introduced by the defense community in 1981 and expanded to the science community after declassification in 1991[1]. While applications such as high contrast imaging with space telescopes[2,3] and space-based free space optical laser communications exist[4,5], implementation and functional performance assessments of a deformable mirror wavefront control system have not yet been demonstrated in orbit, at least, not on a civilian mission[6,7]. The proposed CubeSat Deformable Mirror Demonstration (DeMi) will take a first step toward incorporation of small, low-power, high actuator count deformable mirror wavefront control systems on spacecraft for use in high-performance space telescope and free space laser communication systems.

1.1 Motivation

Applications for wavefront control systems in space can be grouped into four general categories, (i) systems that take images through the Earth's turbulent atmosphere, (ii) systems that transmit and receive laser signals through the Earth's turbulent atmosphere, (iii) systems that take high contrast and high dynamic range images of other objects in space, or (iv) systems that transmit laser signals to and receive laser signals from other objects in space. In addition to their use for wavefront control and correction, deformable mirrors can also be used as the amplitude or phase modulators that code the transmitted signals in free space laser communication systems.

Adaptive optics systems that compensate for atmospheric turbulence (Fried parameter r_0 and Greenwood frequency τ_0) are typically designed to perform with higher speeds and larger strokes than wavefront control systems that do not compensate for atmospheric turbulence. A two-mirror woofer-tweeter (coarse-fine) wavefront control approach is frequently used[8], where the woofer corrects slower, larger amplitude, lower-frequency components and the tweeter corrects faster, smaller-amplitude, higher-frequency components. The DeMi demonstration mission focuses on developing a low-cost, easy-access-to-space platform for validating technologies used for the tweeters: more complex, higher actuator count deformable mirrors.

Direct imaging of exoplanets is an example of a challenging new high contrast ($\sim 10^{10}$), high dynamic range observation that seeks to identify an Earth-like planet around another star in the local solar neighborhood by measuring atmospheric absorption features in its reflected-light spectrum[9]. It is desirable to use a space telescope for Earth-like exoplanet observations (as opposed to observations of larger and brighter gas or ice giant exoplanets), because even for ground-based telescopes with high performance adaptive optics systems[10] and an ideal coronagraph, the speed of atmospheric turbulence and the limited number of photons from the exoplanet target, in addition to constraints on viewing geometry and integration time, limit the achievable contrast. Observations that can capture features in the atmospheric spectra of

Space Telescopes and Instrumentation 2012: Optical, Infrared, and Millimeter Wave, edited by Mark C. Clampin, Giovanni G. Fazio, Howard A. MacEwen, Jacobus M. Oschmann, Jr., Proc. of SPIE Vol. 8442, 84424F
 · doi: 10.1117/12.926681

an Earth-like exoplanet require wavefront control because even a well-engineered space telescope with a sophisticated high performance coronagraph[11,12] will have mid and high spatial frequency wavefront aberrations that will degrade the achievable image contrast[13,14,15]. Drifts in the optics shapes over the long integration times necessary for such a scientific observation should be comparatively small and slow, thus wavefront control techniques can be used to reduce the phase errors to an acceptable level (for example, less than 1 nm). Wavefront control systems are also needed to manage speckles that result from diffraction, phase errors, and noise. In cooperation with the spacecraft attitude determination and control system (ADCS), wavefront control systems can also be used to address sub-milliarcsecond pointing errors.[16]

The development of a space telescope equipped with a high performance coronagraph and deformable-mirror wavefront control system that is capable of the 10^{10} contrast needed to directly image Earth-like exoplanets is expected to be on the order of several hundreds of millions of dollars to over a billion dollars. The goal of the CubeSat Deformable Mirror Demonstration is to provide a low-cost way to quickly test small, low-power, higher actuator-count deformable mirror technologies on-orbit. While several important environmental tests can be performed using these mirrors on the ground (thermal vacuum, vibration, life cycle testing, radiation), it is important to demonstrate that simple wavefront control systems utilizing new deformable mirror technologies have stable, well-calibrated, and predictable performance on orbit. This is particularly important to emphasize, as there is no opportunity to "tweak" or "adjust" a wavefront control system on orbit after launch. It is of particular importance to fully develop robust flight software to control these mirrors and systems; to incorporate them as sensors with spacecraft attitude determination and control systems (ADCS), estimators, and fine pointing algorithms; and to determine how best to capture performance and calibration data along with science observations and transmit it to the ground.

1.2 CubeSat Background

The CubeSat form factor was developed by California Polytechnic Institute (CalPoly) and Stanford University in 1999. It interfaces with a common secondary payload deployer, the Poly-picosatellite Orbital Deployer (P-POD), which significantly reduces the cost and time for obtaining launch opportunities for nanosatellites. The basic nanosatellite unit is a 10 x 10 x 10 cm cube (called 1U). The P-POD unit will support a 3U volume in a variety of combinations.[17] For example, it can accommodate three 1U CubeSats. Or, it can accommodate a single triple-long 3U CubeSat (which can be about 34.05 cm long instead of 30 cm, since space allocated for "feet" separating individual 1U CubeSats can be allocated to the volume of the single 3U). CubeSats are usually launched as secondary payloads on government or commercial primary missions, with their launch accommodation often sponsored by government agencies, such as the NASA Educational Launch of Nanosatellites (ELaNa) program. A 3U CubeSat is an appropriate platform for the DeMi mission because it enables a comparatively quick, simple, low-cost approach for a technology demonstration that would have significant impacts on the design, scale, and capabilities of future space-based optical systems.

2. DeMi PAYLOAD

The purpose of this section is to describe how a 3U CubeSat can be used as a test platform for a simple deformable mirror technology demonstration that increases the technological readiness level (TRL) of a miniaturized, low-power, standalone wavefront control system for space telescope or free space laser communication system applications. While the initial demonstration mission design is kept as simple as possible, it is developed with the goal of increasing complexity and functionality for follow-on missions.

2.1 Payload Overview

For the initial demonstration mission, the goal is to use as much existing commercial off the shelf (COTS) hardware as possible, making modifications as needed for operation in space, and to keep the design as simple as possible. The simple purpose of the payload is to demonstrate that the deformable mirror can be commanded and controlled on-orbit, to characterize its performance, and to show that its on-orbit behavior is understandable and predictable. This goal can be accomplished using an internal coherent light source such as a laser diode, a deformable mirror, and a small number of static optical elements including a beamsplitter, a couple of collimating and focusing lenses, and a detector. For example, the current payload design is the Michelson interferometer layout depicted in Figure 1.

Figure 1 shows a Michelson interferometer sensing approach to demonstrate the functionality of a MEMS DM. The light from the source, S, is divided by a beam splitter (BS) oriented 45 degrees to the beam. The transmitted beam travels to the MEMS deformable mirror where it is reflected back to the beam splitter. Half of this beam is deflected by 90 degrees at the BS and strikes the detector. The reflected beam travels to a flat mirror, M2, where it is reflected back to the beam

splitter. Half of it then passes straight through BS and reaches the detector. The two beams that are directed towards the detector interfere to produce fringes that are analytically well understood as a function of beam coherence/divergence and mirror shape (tip/tilt)[21] and that can be simulated for a variety of other different mirror shapes and positions. Additional collimating and imaging lenses are not shown in Figure 1(a). Figure 1(b) shows an example geometrical optics relationship between the deformable mirror tip/tilt and the beamsplitter exit angle, used in ongoing analyses to consider trades in mirror strok, mirror placement, and the selection of a lens for the detector. For basic piston and tip/tilt modes, it is straightforward to determine how well the deformable mirror is performing by studying the fringes in the images captured by the detector. For example, if the entire deformable mirror surface tilts by an angle θ from its original normal, the observed fringes occur at intervals of $\Delta x' = 2\lambda/\sin(\theta)$. If the deformable mirror surface moves forward (piston) by distance Δd, the observed fringe pattern moves as Δd changes, and the number of fringes that cross the center of the screen is $n = 2\Delta d/\lambda$. Further modeling needs to be done to determine which shapes on the mirror surface are most easily detectable and identifiable.

2.2 Payload design trades

While in future applications it is desirable to use the deformable mirror to make observations of more interesting source objects, such as stars or the Sun or Earth, and to incorporate control of the deformable mirror into the ADCS system, for the moment an internal light source that does not contribute any external pointing requirements is the simplest way to achieve the first goal of demonstrating DM functionality in hardware and software on orbit.

There are several different wavefront sensors that could be implemented other than a Michelson interferometer, including other shear wavefront sensor configurations such as a single shear prism or a Shack-Hartmann wavefront sensor. Wavefront sensors that perform best when used with an actuated element, such as a pyramid or curvature wavefront sensor, carry additional risk and complexity in the actuated element and are not considered for this initial demonstration. The incorporation of a lenslet array on the detector for a Shack-Hartmann wavefront sensor may be a worthwhile trade in complexity versus detection sensitivity and will receive further consideration during the design process.

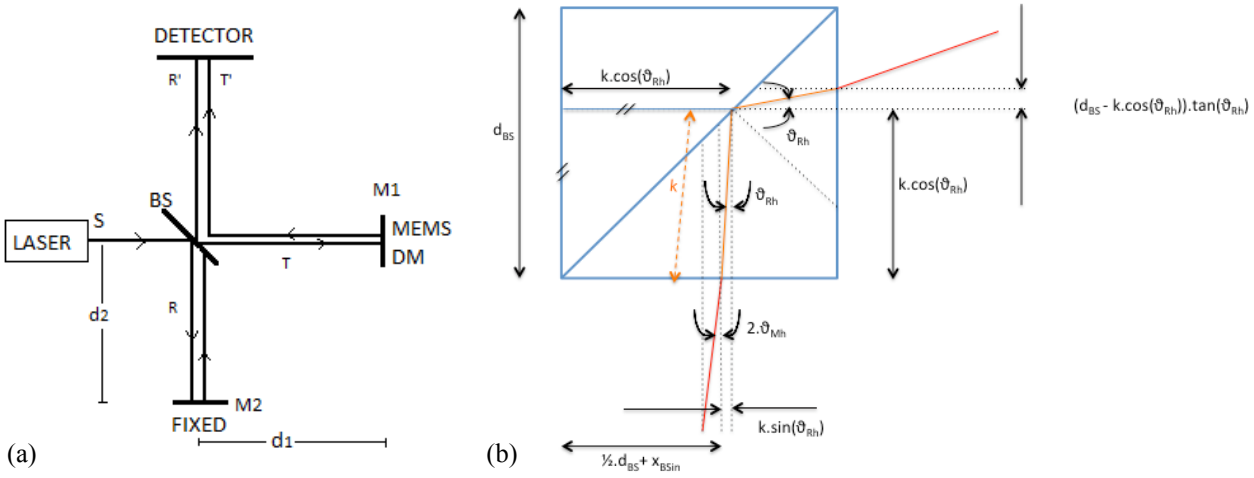

Figure 1(a): Michelson interferometer approach to demonstrate the functionality of a MEMS DM. The light from source, S, is divided by a beam splitter (BS) oriented 45 degrees to the beam. The transmitted beam travels to the MEMS deformable mirror where it is reflected back to the beam splitter. Half of the beam is deflected by 90 degrees at BS and strikes the detector. The reflected beam travels to M2 where it is reflected and half of it then passes straight through BS and reaches the detector. The two beams that are directed towards the detector interfere to produce fringes that are analytically well understood as a function of beam coherence/divergence and mirror tip/tilt[21] and that can be simulated for a variety of other different mirror shapes. Additional collimating and camera lenses not shown. 1(b): Example geometrical optics relationship of deformable mirror tip/tilt on exit angle, used in an ongoing study to optimize the component placement and mirror stroke selection.

Even though the mirrors themselves are quite small, a widely acknowledged challenge to incorporating high actuator count deformable mirror systems on a spacecraft is the substantial size, mass, volume, power, and complexity of the mirror driver boards and wire harnesses. While development of application-specific integrated circuit (ASIC) drivers is a current focus of several deformable mirror manufacturers,[18,19] it is uncertain when the ASIC drivers will become generally available and whether they will be usable for space applications. In the meantime, one candidate DM has been identified for which both the DM and existing drive electronics should fit in the remaining ~1.3U payload volume (after supporting bus systems are accounted for) of a 3U CubeSat without significant modification. The current DeMi payload design accommodates a "Mini" deformable mirror from the Boston Micromachines Corporation (BMC). The BMC Mini is a 6 x 6 deformable mirror (32-actuator, as the four corners are not active). There are three different stroke and aperture options with the Mini[20], as summarized in Table 1. A trade study is underway to determine which of these options would be best.

Table 1: Boston Micromachines Mini MEMS deformable mirror options[20]

Stroke	1.5 µm	3.5 µm	5.5 µm
Aperture	1.5 mm	2.0 mm	2.25 mm
Pitch	300 µm	400 µm	450 µm
Approx. Mechanical Response Time (10%—90%)	20 µs	100 µs	500 µs
Approx. Interactuator Coupling (+/-5%)	15%	13%	22%

The Mini DM has 14 bit step resolution and a sub-nm average step size. The fill factor is >99%, the surface finish is < 20 nm RMS, and the driver is completely powered and controlled by a USB 2.0 interface. The frame rate is 8 kHz, with a 34 kHz burst mode. For the DeMi mission, the most recently available BMC Mini packaging format is selected (5 cm diameter and 2.21 cm tall, 75 g without cables). The existing driver board has dimensions of 13 x 10 x 1.8 cm, and there is bare, unused printed circuit board (no traces) for ~2.75 mm on each side of the width dimension, such that the board could have dimensions 13 x 9.5 x 1.8 cm. The initial plan is to use this board and make as few modifications as possible, apply conformal coating, stake and secure connectors.

2.3 Concept of Operations

The use of an internal light source for the initial demonstration of DM functionality on-orbit eliminates any payload-specific requirements on the CubeSat's altitude and inclination. The orbit altitude range of 300 to 500 km is limited on the high side by the CubeSat maximum de-orbit time requirement and on the low side by drag and the desired mission lifetime of one year. A high-level overview of the concept of operations includes phases for launch, deployment, and detumbling, thirty days of commissioning, and a success threshold of one month of nominal operations and data downlink with a goal of ten months of nominal operations and data downlink. The first phase of nominal operations involves open-loop wavefront sensing of a repeating sequence of mirror surface shapes during which calibration is performed. This is followed by the second phase of the mission, closed-loop wavefront sensing, where the CubeSat microcontroller is used to achieve and maintain a desired surface shape on the DM. This is followed by a third phase whose purpose is to simulate the effects of bad actuators and increasingly noisy signals before deorbiting.

3. CUBESAT SUBSYSTEMS

3.1 Power

Two solar panel configurations were modeled in STK: (i) a set of four 3U body-mounted panels, shown in Figure 4, and (ii) a set of four two-sided 3U deployed solar panels and no body-mounted panels. Each 3U surface holds 7 ultra-triple junction solar cells. In each case, the spacecraft is oriented with the long axis parallel to the zenith-nadir line. The results from power generation calculations for a series of orbital altitudes and inclinations for each configuration for one orbit are shown in Figures 2 and 3.

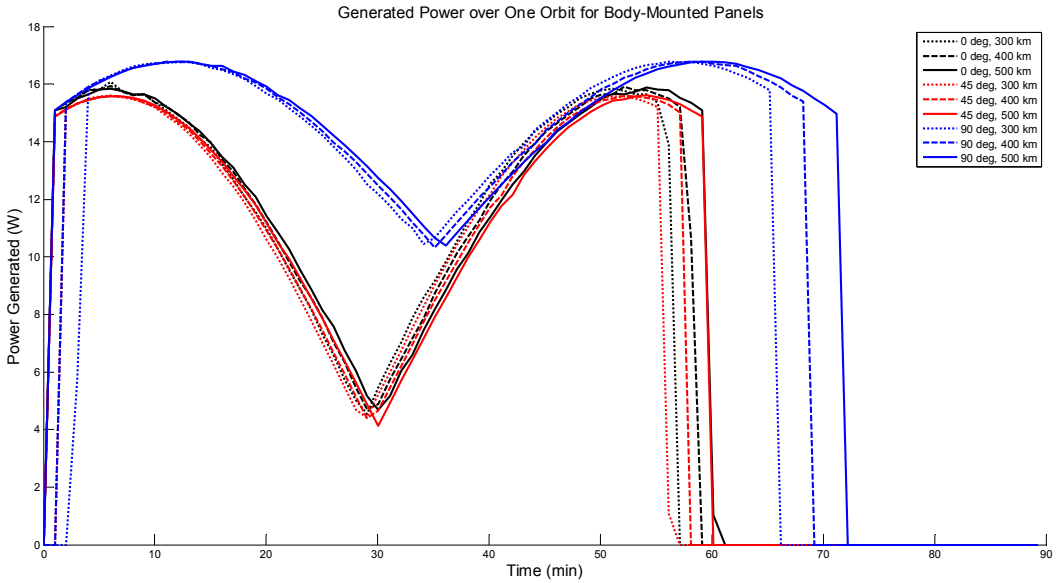

Figure 2: Power generated by 3U body-mounted solar panels over the course of an orbit.

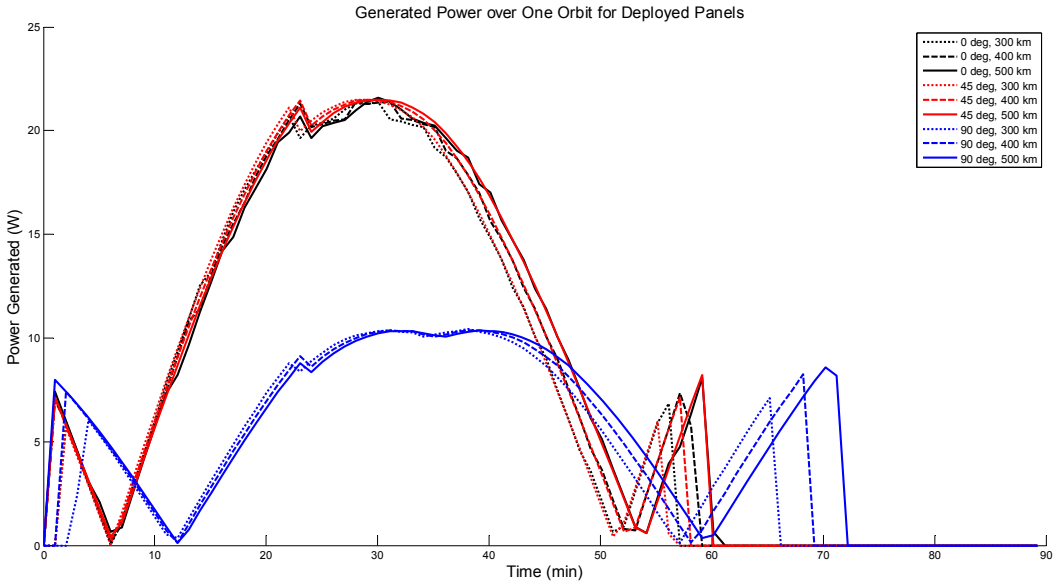

Figure 3: Power generated by four two-sided 3U deployable solar panels over the course of an orbit.

Figures 2 and 3 show that the while peak power generation is generally higher with the deployed panels, the body-mounted panels provide more uniform power generation pattern across the orbit. Table 2 compares the orbit-averaged power (averaged over daylight, non-zero power generation) for each case.

Table 2: Orbit average generated power

Orbital Inclination (degrees)	Orbital Altitude (km)	4 x 3U Body-Mounted Panels Orbit Avg. Generated Power (W)	4 x two-sided 3U Deployed Panels Orbit Avg. Generated Power (W)
0	300	12.3	12.0
0	400	12.4	11.9
0	500	12.2	11.8
45	300	11.9	12.1
45	400	12.2	12.1
45	500	12.2	12.1
90	300	14.8	6.2
90	400	15.0	6.4
90	500	15.0	6.4

While the peak power generation is higher with the deployed solar panel configuration, a calculation of the orbit-averaged power shows that the body-mounted panel generation is more favorable than that of the deployed panels for the a mission where the body-mounted solar panels will not be obstructed, for example, due to the presence of an antenna, sensor, or instrument field of view. Using only deployed panels does not provide a significant increase in power generation, it makes for a less consistent power profile, and deployed panels add unnecessary complexity and cost to the spacecraft. For these reasons, the current design utilizes four 3U body-mounted panels.

If further analysis shows that more power generation is required, additional options can be considered. One is to utilize deployed panels in conjunction with body-mounted panels. Another is to design the spacecraft to enable solar array sun-tracking, which would require a more robust ADCS design, articulated solar panels, or both.

3.2 Structure

The basic structure of the spacecraft is a 3U CubeSat with body-mounted solar panels. Figure 4 shows two views of the spacecraft: one showing the 3U skeleton with volume-representative parts, and one showing the outer solar panel structure.

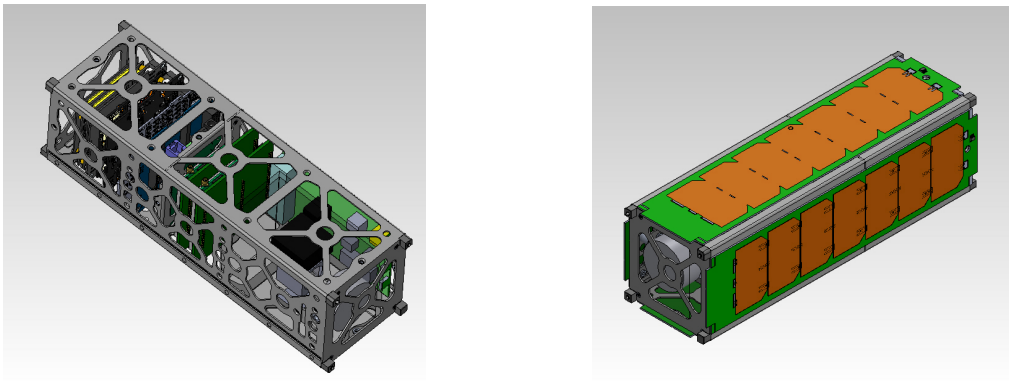

Figure 4: All components will be housed inside a 3U CubeSat (left) with body-mounted solar panels covering the outer walls (right). Antennas for communication would be mounted on the top and bottom of the structure, which would be maintained in a gravity gradient orientation (with either the top or bottom end nadir pointing).

A preliminary placement of the subsystem boards and payloads within the 3U CubeSat volume is shown in Figure 5. The microcontroller and motherboards are from Pumpkin Inc., the batteries and electrical power system (EPS) are from Clyde Space, and the structure is a Pumpkin 3U skeletonized chassis. The two communications boards have redundant functionality at different frequencies, one at VHF/UHF and one at S-band. There are several suppliers of VHF/UHF CubeSat transceivers, such as Clyde Space and AstroDev, and the S-band transceiver would either be an Espace Payload Telemetry System (2.0 to 2.3 GHz) or an Microhard Systems MHX modem operating in the 2.4 GHz band. The payload takes up a volume of approximately 1.3U.

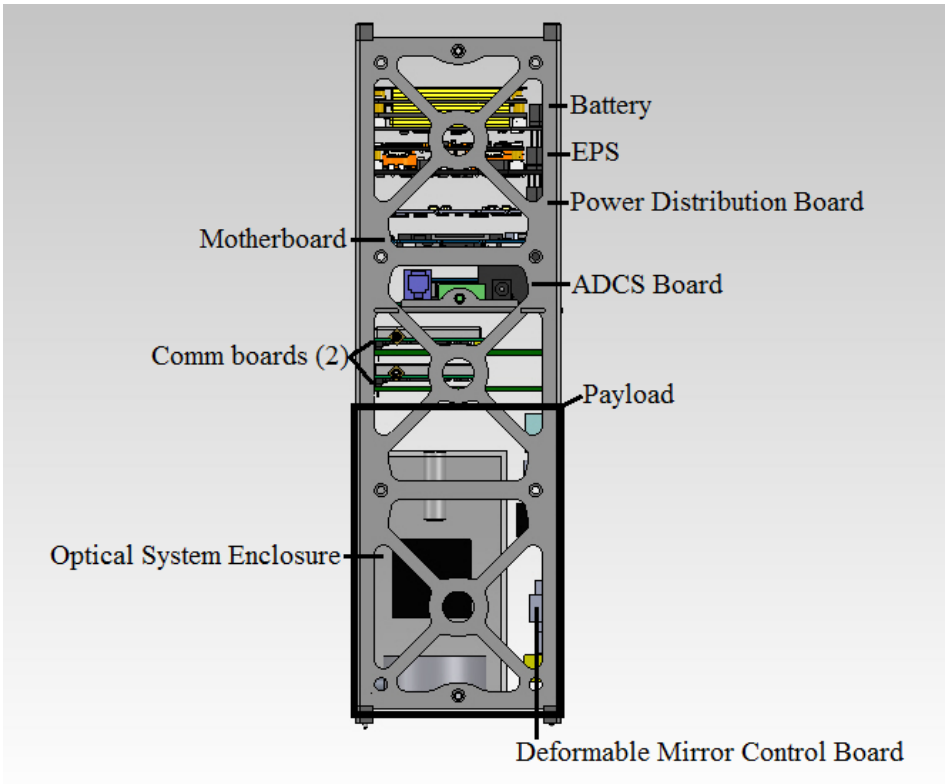

Figure 5: Stack and payload accommodation in the 3U DeMi CubeSat.

3.3 ADCS

The Attitude Determination and Control System (ADCS) for the initial DeMi design needs only to achieve pointing toward a ground station for communication. The payload is housed entirely within the bus structure and its operability is not affected by the attitude or orientation of the spacecraft (although sensitivity to disturbances is another area under study). Referencing examples flown on previous CubeSat missions[22], a simple approach for the ADCS system is passive magnetic control. A sensor package of a magnetometer, IMU, and sun sensors satisfy the relatively flexible pointing requirements of this mission.

Follow-on missions to DeMi would take the next steps to include an outward-looking camera and develop flight software that incorporates control of the DM with the ADCS system to achieve finer pointing requirements and tighter stability. Such future missions could also build upon the initial DeMi platform and incorporate additional sensors such as Earth horizon sensors and a global positioning system (GPS) receiver, as well as active control systems by including magnetorquers, reaction wheels, or microthrusters.

3.4 Thermal

The baseline thermal design is a passive system with the exception of the Clyde Space battery, which includes internal heaters. A comprehensive thermal model of the satellite and a more in-depth analysis of the payload components will determine the need for active thermal management. Small flexible heater circuits, such as those from Minco, may be required for spot thermal management, such as near the Thorlabs CPS405 laser diode (however, the CPS405 is engineered to survive -40 to 80°C and operate in -10 to 40° C).

3.5 Communications

The communications system will include two transceivers, one VHF/UHF and one S-band. Redundant antennas for each transceiver are located on the “top” and “bottom” of the bus structure, one of which will be nadir pointing. There are

several commercial options for CubeSat VHF/UHF transceivers as well as ground stations and support from the amateur radio community. Two options are currently being considered for the S-band transceiver. The first option is an Espace Payload Telemetery System (PTS) operating in the 2.0 to 2.3 GHz range and using the recently refurbished Open System of Agile Ground Stations (OSAGS) facilities at Kwajalein, Cayenne, and Singapore. The OSAGS system has a control center on MIT campus as the same ground station locations were previously used to support the NASA High Energy Transient Explorer (HETE-2) mission. This option would work best with a lower-inclination orbit since the ground stations are all near-equatorial. The second option is to use a Microhard MHX modem at 2.4 GHz and identify appropriate partner ground stations. Having a set of two transceivers both builds redundancy into the onboard system and helps to ensure that the payload can communicate with ground stations while tumbling by increasing the number of ground stations that it is compatible with. The VHF/UHF bandwidth would allow DeMi to take advantage of a global network of amateur radio ground stations to track, send commands, and receive telemetry data. The S-band radio would be used for science data downlink.

3.6 Payload accommodation in the 3U CubeSat

Figure 6 shows a preliminary selection of primary components for the DeMi payload and identifies a part for each of the functions shown in the schematic in Figure 1(a). The collimated laser diode is the CPS405 from Thorlabs, a 4.5 mW, 405 nm laser which takes 5 VDC regulated power and has a large survivable temperature range. The beamsplitter (CM1-BS013) is also from Thorlabs, a cube-mounted, non-polarizing beamsplitter weighing about 136 g (0.3 lbs.). The BMC 6 x 6 (32 actuator) Mini deformable mirror options are summarized in Table 1. The flat mirror is also from Thorlabs (PFSQ10-03-F01) and weighs about 28 g. The current camera selection is an 8-bit 1/3" CMOS (Aptina) Imaging Development Systems (IDS) UI-1646 LE with an S lens mount. The IDS UI-1646 LE weighs 12 g and is normally USB powered. The resolution is 1280 x 1024 and with an optical size of 4.608 x 3.686 mm and pixel pitch of 3.6 μm.

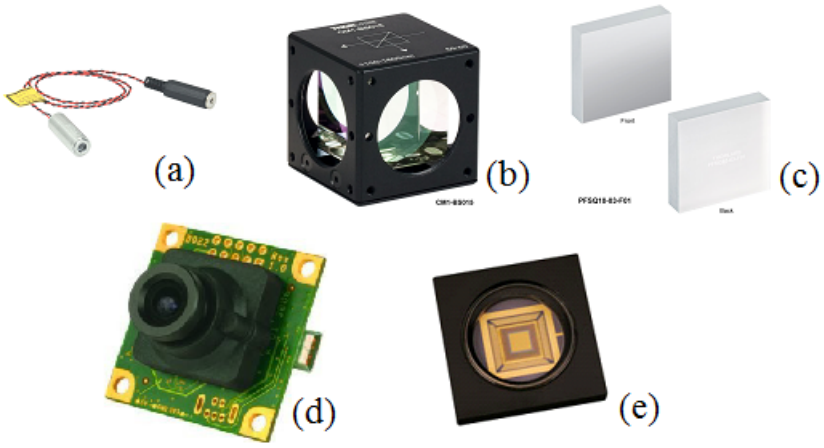

Figure 6: DeMi preliminary payload components: (a) CPS405 laser diode from Thorlabs, (b) CM1-BS013 beamsplitter from Thorlabs, (c) flat mirror from Thorlabs, (d) CMOS detector from Imaging Development Systems (IDS) PFSQ10-03-F01, and (e) deformable 6 x 6 (32-actuator) Mini deformable mirror from BMC.

Figure 7 shows the layout and scale of the system housed in the optical shroud (shown in a side view in Figure 5). Final selection of a lens for the camera is a function of how much stroke the deformable mirror will have and what fraction of the detector it is desirable to illuminate.

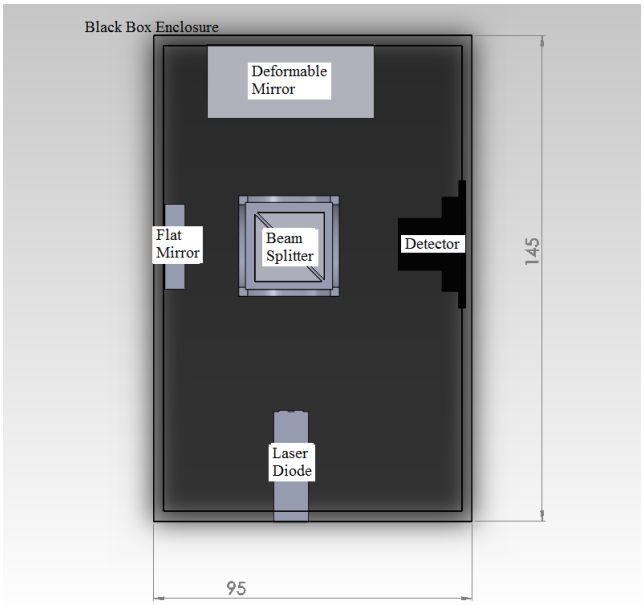

Figure 7: Placement of optical components in payload volume (dimensions are in mm). The components are mounted to and housed within a black box to eliminate reflection and interference from the spacecraft bus. The current layout (still subject to change) has 35.4 mm from the laser to the near edge of the beam splitter, 16.5 mm from the flat mirror to the near edge of the beam splitter, 16.6 mm from the detector to the near edge of the beam splitter, and 23.8 mm from the DM to the near edge of the beam splitter.

4. SUMMARY AND FUTURE WORK

4.1 Summary

In this paper, we have shown that it is feasible to design a 3U CubeSat platform that can accommodate a MEMS deformable mirror demonstration experiment using COTS and CubeSat parts and components. Development of both a software model that generates simulated observations for a variety of shapes commanded to the DM as well as a hardware lab bench test of the payload performance is in progress. A successful CubeSat deformable mirror demonstration mission would demonstrate simple open loop and closed loop control of a 32-actuator BMC MEMS DM on orbit, enable follow-on missions to test other DMs and driver technologies on a similar platform, and encourage follow-on missions with more sophisticated outward-looking imaging optics and pointing control algorithms.

4.2 Future work: DeMi

Several trade studies need to be completed using a higher fidelity model of the optical elements and wavefront sensing system for DeMi. One of the primary trades is to determine which of the 1.5 µm, 3.5 µm, or 5.5 µm stroke Mini DMs is most compatible with the scale of the beamsplitter and lens/detector. Further effort is also needed to evaluate the power consumption of a continuously running experiment and determine whether it will be duty cycled or not. In developing the interface between the microcontroller and the mirror, it is desirable to start to incorporate the mirror as a sensor for the ADCS system.

4.3 Future work: Follow-on missions

There are several different follow-on opportunities that could be pursued as a result of this simple deformable mirror demonstration. One of the more interesting options would be to use the same platform for a different small deformable mirror and driver for comparison. Next steps would involve incorporating a compact external-viewing camera system that is imaging (and tracking) an astronomical object. The long-term goal is to promote the use of small deformable mirrors for space imaging and free space communication applications on any size payload and spacecraft.

ACKNOWLEDGMENTS

The authors would like to acknowledge support from the NASA Office of the Chief Technologist NASA Space Technology Research Fellowships (OCT-NSTRF), the MIT International Science and Technology Initiatives (MISTI), and the MIT Undergraduate Research Opportunities Program (UROP). The authors also appreciate insightful discussions with Michael Feinberg, Dr. Steven Cornelissen, and Dr. Paul Bierden at Boston Micromachines, Inc., Dr. Wes Traub and Dr. John Trauger at NASA JPL, Prof. N. Jeremy Kasdin and Tyler Groff at Princeton University, Dr. Ruslan Belikov at NASA Ames Research Center, Dr. Xiaoli Sun at NASA Goddard Space Flight Center, Dr. David E. Smith, Prof. Maria T. Zuber, Prof. David Miller, and Matt Smith at MIT, Dr. Don Gavel and Andrew Norton at UCSC, Dr. Bruce Macintosh at LLNL, Dr. Jason Stewart at MIT Lincoln Laboratory, and Prof. Mikhail Vorontsov at the University of Maryland.

REFERENCES

[1] Duffner, R., [The Adaptive Optics Revolution: A History] Albuquerque: University of New Mexico Press, 457 pp. (2009).
[2] Cahoy, K., O. Guyon, G. Schneider, M. Marley, R. Belikov, M. Meyer, S. Ridgway, W. Traub, and N. Woolf, "Science performance of the Pupil-mapping Exoplanet Coronagraphic Observer (PECO)," Proc. SPIE, 74400, 12 pages, doi:10.1117/12.826608 (2009).
[3] Guyon, O., J.R.P. Angel, R. Belikov, R. Egerman, D. Gavel, A. Giveon, T. Greene, K. Cahoy, B. Kern, M. Levine, S. Ridgway, S. Shaklan, D. Tenerelli, R. Vanderbei, R. Woodruff, "Detecting and characterizing exoplanets with a 1.4-m space telescope: the Pupil-mapping Exoplanet Coronagraphic Observer (PECO)," Proc. SPIE, 74400, doi:10.1117/12.826350 (2009).
[4] Smith, D.E., M.T. Zuber, X. Sun, G.A. Neumann, J.F. Cavanaugh, J.F. McGarry, T.W. Zagwodzki, "Two-way laser link over interplanetary distance," Science, 311(5757), 53, doi:10.1126/science.1120091 (2006).
[5] Ting, C., D.G. Voelz, M.K. Giles, "Laser satellite communications with adaptive optics," Proc. SPIE 5892, doi: 10.1117/12.620905 (2005).
[6] Mendillo, C., Chakrabarti, S., Cook, T., and Hicks, B., "Flight demonstration of a milli-arcsecond optical pointing system for direct exoplanet imaging," American Astronomical Society, AAS Meeting #219, #446.03 (2009).
[7] Achenbach, J., "NASA gets two military spy telescopes for astronomy," The Washington Post, 4 June 2012, <http://www.washingtonpost.com/national/health-science/nasa-gets-military-spy-telescopes-for-astronomy/2012/06/04/gJQAsT6UDV_story.html> (accessed 4 June 2012).
[8] Correia, C., H.-F. Raynaud, C. Kulcsar, J.-M. Conan, "On the optimal reconstruction and control of adaptive optical systems with mirror dynamics," JOSA A, 27(2), 333-349, doi:10.1364/JOSAA.27.000333 (2010).
[9] Kasdin, N.J., et al., "Extrasolar planet finding via optimized apodized pupil and shaped pupil coronagraphs," Ap.J. 582, 1147 (2003).
[10] Angel, R. "Ground based imaging of extrasolar planets using adaptive optics," Nature, 368, 203-207, doi:10.1038/368203a0 (1994).
[11] Kuchner, M. and W. Traub, "A coronagraph with a band-limited mask for finding terrestrial planets," Ap.J. 570, 200 (2002).
[12] Sivaramakrishnan, A., et al., "Speckle decorrelation and dynamic range in speckle noise limited imaging," Ap.J. 581, L59 (2002).
[13] Perrin, M., et al. "The structure of the high strehl ratio point-spread functions", Ap.J. 596, 702 (2003).
[14] Macintosh, B., et al, "The Gemini Planet Imager: From science to design to construction", 2008 Proc. SPIE 7015-18
[15] Guyon, O. et al. "Exoplanet imaging with a Phase-induced Amplitude Apodization Coronagraph. I. Principle," Ap. J., 622, 744, doi: 10.1086/427771, (2005).
[16] Guyon, O., Matsuo, T. and Angel, R.,"Coronagraphic Low-Order Wave-Front Sensor: Principle and application to a Phase-Induced Amplitude Apodization coronagraph", Ap.J., 693, 75, (2009).
[17] Puig-Suari, J., C. Turner, R.J. Twiggs, "CubeSat: The development and launch support infrastructure for eighteen different satellite customers on one launch," 15th annual Utah State University SmallSat Conference, SSC01-VIIIb-5 (2001).

[18] Stewart, J., et al. “Compact low power driver for deformable mirror systems,” NASA 2009 SBIR solicitation proposal, <http://sbir.gsfc.nasa.gov/SBIR/abstracts/09/sbir/phase2/SBIR-09-2-S2.02-9229.html> (accessed 5 June, 2012).
[19] Wu, X., L. Yao, and H. Ou, “Novel hierarchically-dimensioned deformable mirrors with integrated ASIC driver electronics,” Proc. SPIE, 8253, 82530A-2 (2012)
[20] Boston Micromachines Corporation, <http://www.bostonmicromachines.com/light-modulator.htm> (accessed 5 June, 2012).
[21] Demtroeder, W., “Laser spectroscopy, basic concepts and instrumentation,” Springer-Verlag, Berlin, Heidelberg, New York, 3rd edition, 122-127 (2003).
[22] Springmann, J., et al. “The attitude determination system of the RAX satellite.” Acta Astronautica, 75, 120-135 (2012).